Manuscript type: Original research

Title: Preoperative tumor texture analysis on MRI predicts high-risk disease and reduced survival in endometrial cancer.

Abstract

Purpose:

To explore whether tumor texture parameters from preoperative MRI are related to known prognostic clinical and histological features (deep myometrial invasion, cervical stroma invasion, lymph node metastases and high-risk histological subtype) and to outcome in endometrial cancer patients.

Materials and Methods:

From April 2009 to November 2013 preoperative pelvic MRI (1.5T) including contrast-enhanced T1-weighted (T1c), T2-weighted (T2) and diffusion-weighted imaging (DWI) was performed in 180 patients with endometrial carcinoma, prospectively included under institutional review board approval. Tumor regions of interest (ROIs) were manually drawn on the slice displaying the largest cross-sectional tumor area, using the proprietary research software TexRAD for analysis. With filtration-histogram technique, the texture parameters standard deviation, entropy, mean of positive pixels (MPP), skewness and kurtosis were calculated. Associations between texture parameters and clinical and histological features were assessed by uni- and multivariable logistic regression, including models adjusting for preoperative biopsy status and conventional MRI findings. Multivariable Cox regression analysis was used for survival analysis.

Results:

High tumor entropy in apparent diffusion coefficient (ADC)-maps independently predicted deep myometrial invasion (OR 3.2, p<0.001), and high MPP in T1c images independently predicted high-risk histological subtype (OR 1.01, p=0.004). High kurtosis in T1c images predicted reduced recurrence- and progression-free survival (HR 1.5, p<0.001) after adjusting for MRI-measured tumor volume and histological risk at biopsy.

Conclusion:

MRI-derived tumor texture parameters independently predicted deep myometrial invasion, high-risk histological subtype and reduced survival in endometrial carcinomas, and thus, represent promising imaging biomarkers providing a more refined preoperative risk assessment that may ultimately enable better tailored treatment strategies in endometrial cancer.

Keywords:

Endometrial Neoplasms

Magnetic Resonance Imaging

Image Analysis, Computer-Assisted

Entropy

Risk Assessment

Introduction

Tumor heterogeneity is a key feature of malignant disease. Several pan-cancer analyses, comprising a variety of cancer types, have reported intra-tumor genetic heterogeneity to be associated with tumor aggressiveness and reduced survival (1, 2). Mechanisms proposed to explain the aggressive behavior of heterogeneous tumors include Darwinian selection among clones enabling tumor adaption and drug-resistance (3).

Texture analysis (TA), a method for quantification of heterogeneity in images, has become an important element in the growing field of radiomics, the science of high-throughput extraction of quantitative features from radiological imaging data (4). Although radiomics inherently operates at a more macroscopic level than genomics and histological markers, the method has proven useful in medical diagnostic imaging, especially in oncological imaging (5). Magnetic resonance imaging (MRI)- and computed tomography (CT)-derived texture parameters have been proposed as tools for accurate diagnosis, preoperative risk stratification or assessment of treatment response in several cancer types, e.g. in the brain (6), lung (7), breast (8) and prostate (9). A recent preliminary study also reported MR texture analysis (MRTA) as a useful tool for preoperative risk stratification in endometrial cancer (10).

Endometrial cancer is the most common gynecologic malignancy in industrialized countries, and the incidence is increasing (11). Treatment strategy and prognosis are traditionally based on the International Federation of Gynecology and Obstetrics (FIGO) stage and histological subtype and grade determined from the hysterectomy specimen (12, 13). To enable more individualized surgical treatment, improved methods for preoperative risk stratification methods are highly warranted.

MRI is widely used for preoperative assessment of endometrial cancer (14-16). However, conventional MRI has confirmed shortcomings in predicting FIGO stage (16, 17), and interobserver variability between radiologists also represents a source of inaccuracy (18).

Advances in MRI technology, including functional MRI techniques, e.g. diffusion weighted imaging (DWI), dynamic contrast enhanced (DCE)-MRI and MR spectroscopic imaging (MRSI), can to an extent reduce the subjectivity in the assessment of endometrial cancers and yield novel biomarkers for preoperative risk stratification. Still, overtreatment at primary surgery (e.g. unnecessary lymphadenectomy in low-risk patients) may represent a problem. In this regard, MRTA could potentially enhance the role of diagnostic imaging and refine the preoperative risk assessments.

This large, population-based study aimed to explore whether the staging parameters deep (≥50%) myometrial invasion (DMI), cervical stroma invasion (CSI) and lymph node metastases (LNM), high-risk histological subtype and clinical outcome in endometrial cancer patients, are reflected in MRTA parameters.

Materials and Methods

Study setting

This prospective study was conducted under institutional review board approval with written informed consent from all patients. From April 2009 to November 2013 preoperative pelvic MRI was performed in a population-based cohort of 216 consecutive patients with endometrial carcinoma histologically verified at subsequent staging. Imaging data from 180 cases were found eligible for further analysis (see section ‘Image analysis’). All patients were diagnosed and treated at the same university hospital, which is a European Society of Gynaecologic Oncology accredited center. The last follow-up was in January 2017 and mean follow-up time for the group of patients without recurrence or progression was 51 months (range 0-85).

Histological diagnosis

All patients were surgicopathologically staged according to the 2009 FIGO staging system (12). Hysterectomy specimens were sectioned along the longitudinal plane of the uterus, and myometrial invasion and cervical stromal invasion were estimated grossly and confirmed microscopically according to standard criteria (19).

Imaging protocol

MRI was performed on a 1.5T Siemens Avanto running Syngo MR B17 (Erlangen, Germany) using a six-channel body coil. Prior to imaging, 20 mg butylscopolamine bromide (Buscopan, Boehringer, Ingelheim, Germany) was administered intravenously.
Largely based on Guidelines of the European Society of Urogenital Imaging (ESUR) (15), the MRI protocol included pelvic sagittal and axial oblique (perpendicular to the long axis of uterus) T2-weighted images and axial oblique T1-weighted gradient-echo images obtained before and after intravenous contrast administration (Dotarem, Guerbet, Villepinte, France: 0.1 mmol gadolinium per kilogram of body weight, 3 ml/s injection speed) using a 2 minute delay (18). Section thickness was 3 mm for T2 images and 2 mm for T1 images.

Pelvic DWI was acquired using an axial oblique two-dimensional echo planar imaging sequence with b-values of 0 and 1000 s/mm^2, and apparent diffusion coefficient (ADC)-maps were generated with section thickness 5 mm.

Mean (range) interval between MR examination and surgical staging was 11 (0-98) days.

Image analysis

One radiologist (SYH, with 5 years of experience with pelvic MRI) blinded for clinical and histological data, assessed the eligibility of the images for MRTA. Of the 216

scanned patients, 33 were excluded due to small or poorly defined tumors, and three due to major image artefacts. Thus, 180 patients were included for MRTA, three of these had major artefacts at DWI only. Contrast-enhanced T1-weighted images (T1c, n=180), T2-weighted images (T2, n=180) and ADC-maps (n=177) were exported to the commercially available research software TexRAD (TexRAD Ltd, part of Feedback Plc, Cambridge, UK).

Results from conventional MRI (assessment of tumor size, myometrial and cervical invasion and presence of lymph node metastases) were based on independently performed readings by three observers as previously described (20).

Texture analysis

In TexRAD the radiologist manually drew regions of interest (ROIs) separately on T1c images, T2 images and ADC-maps, aiming at including all viable tumor tissue on the slice displaying the largest cross-sectional tumor area (Figure 1). The ROIs were processed using a filtration-histogram technique, in which image elements of different sizes were enhanced corresponding to spatial scale filter (SSF) from 2-6 mm, i.e. fine (2 mm), medium (3-5 mm) and coarse texture (6 mm) (Figure 1). Quantification of texture in tumor ROIs comprised mean intensity, standard deviation (SD), entropy, mean of positive pixels (MPP), skewness and kurtosis. The mean intensity does not reflect heterogeneity per se, and thus, this feature was omitted in further analyses. MPP in unfiltered MR images (SSF=0) equals mean intensity and was also omitted. Thus, the total number of texture parameters included in the statistical analyses was 87 (combinations of T1c/T2/ADC-map, SD/entropy/skewness/MPP/kurtosis at SSF 0/2/3/4/5/6).

Statistical analysis

The majority of texture parameters did not have normal distribution, thus non-parametric tests were used. Mann-Whitney U Test assessed the texture parameters' ability to predict DMI, CSI, LNM and high-risk histological subtype (endometrioid grade 3 or non-endometrioid). The texture parameters were subsequently ranked according to lowest p-value, and the best predictors selected for receiver operator characteristic (ROC)-curve analyses and univariable and multivariable logistic regression. In the multivariable analyses, MRI-measured tumor volume, conventional MRI reading results and preoperative biopsy risk status were adjusted for.

Spearman's bivariate correlation test was used to explore correlations.

Survival analysis was performed with all texture parameters separately in univariable Cox regression analysis for predicting recurrence- and progression-free survival (RPFS), i.e. time to recurrence (for patients considered to be cured by primary treatment) or progression (for patients known to have residual disease after primary treatment). Ranked according to lowest p-value, the best predictor was selected to be included in a multivariable analysis also including MRI-measured tumor volume and preoperative biopsy risk status. For the top ranked texture parameters, differences in RPFS were assessed by the Mantel-Cox test and Kaplan-Meier plots.

The 87 texture parameters tested, were partly highly correlated (Suppl. Table 1-3). Hence, a modified Bonferroni correction was applied, in which the number of effective tests was estimated to 25, yielding a significance level of 0.002. In the multivariable analyses a traditional significance level of 0.05 was used.

The data were analyzed using SPSS 23.0 (IBM, Armonk, NY, USA).

Results

Patients

Mean patient age at primary treatment in the study sample (n=180) was 67 years (Table 1). Primary surgical treatment included bilateral salpingo-oophorectomy and hysterectomy for 98% (177/180), tumor reduction surgery for 1/180 and curettage only for 2/180. Lymphadenectomy was performed in 86% (154/180), pelvic only in 126 patients, pelvic and para-aortic in 28 patients. In patients who underwent lymphadenectomy, the mean number of resected nodes was 18 (range 1-54). Adjuvant therapy was given to 39% (70/180); comprising chemotherapy in 83% (58/70), radiotherapy (external or internal) in 16% (11/70) and hormonal treatment in 1% (1/70). Further details on patient- and tumor characteristics are given in Table 1.

Overall evaluation of texture parameters

Entropy, followed by MPP and kurtosis, had the highest proportion of tumor texture parameters significantly predicting deep myometrial invasion, cervical stroma invasion, lymph node metastases and high-risk histological subtype, based on T1c images, T2 images and ADC-maps (Figure 2) at various filter levels (including no filtration). High values of entropy and kurtosis (in T1c images, T2 images and ADC-maps) consistently predicted high-risk features, whereas low values of MPP, skewness and SD in T2 images predicted high-risk features, as opposed to high values in T1c images and ADC-maps (Figure 2). The top ranked texture parameters for prediction of deep myometrial invasion, cervical stroma invasion, lymph node metastases, high-risk histological subtype and recurrence- and progression-free survival, respectively, are given in Table 2.

The texture parameters based on the same MRI sequence and texture feature, i.e. only differing in filter level, were highly correlated (Suppl. Table 1-3). For entropy this was particularly striking, with correlation coefficients ranging from 0.86 to 1.00.

Prediction of deep myometrial invasion (DMI)

Of the 87 texture parameters assessed, 44 significantly ($p<0.002$) predicted DMI in univariable analysis. The majority of these comprised the parameters entropy, MPP and kurtosis, among which the top 10 all comprised entropy (Suppl. table 4). The top ranked predictor of DMI, entropy in ADC-maps at filter level 6 (ADC_Entropy6), independently predicted DMI with an odds ratio of 3.2 (95% confidence interval 1.7-6.1, $p<0.001$) when adjusting for high-risk status based on preoperative biopsy (endometrioid grade 3 or non-endometrioid), conventional MRI reading suggesting DMI, and MRI-measured tumor volume (Table 3). The receiver operator characteristic (ROC)-curve yielded an area under the ADC_Entropy6 ROC-curve (AU-ROC) of 0.81 ($p<0.001$) (Figure 3a) for prediction of DMI.

Prediction of cervical stroma invasion (CSI)

For prediction of CSI in univariable analysis, none of the 87 texture parameters reached the significance level of 0.002. The top ranked predictor of CSI, MPP in T2 images at filter level 4 (T2_MPP4), did not independently predict CSI when adjusting for preoperative biopsy indicating cervical tumor invasion, conventional MRI reading suggesting CSI, and MRI-measured tumor volume (Table 3). The corresponding AU-ROC for T2_MPP4 was 0.64 ($p=0.01$) (Figure 3b) for prediction of CSI.

Prediction of lymph node metastases (LNM)

Five out of 87 texture parameters were significant ($p<0.002$) predictors of LNM in univariable analysis, all five parameters being entropy in T1c images at different filter levels (Suppl. table 4). The top ranked parameter, entropy in T1c images at filter level 6 (T1c_Entropy6), was, however, non-significant in multivariable analysis, when adjusting for

high-risk status in preoperative biopsy, conventional MRI reading suggesting LNM and MRI-measured tumor volume (Table 3). The corresponding AU-ROC for T1c_Entropy6 was 0.73 (p=0.001) (Figure 3c) for prediction of LNM.

Prediction of high-risk histological subtype

Sixteen of the tested 87 texture parameters were significant (p<0.002) predictors of high-risk histological subtype (endometrioid grade 3 and non-endometrioid tumors) in univariable analysis. The majority of these parameters comprised entropy, and the remaining MPP (Suppl. table 4). The top ranked predictor, MPP in T1c images at filter level 4 (T1c_MPP4), independently predicted high-risk histological subtype with an odds ratio of 1.01 (1.00-1.01, p=0.004) when adjusted for high-risk status based on preoperative biopsy and MRI-measured tumor volume (Table 3). The corresponding AU-ROC for T1c_MPP4 was 0.66 (p<0.001) (Figure 3d) for prediction of high-risk histological subtype.

Survival analysis

Thirteen out of 87 texture parameters significantly (p<0.002) predicted recurrence- and progression-free survival (RPFS) in univariable Cox regression analysis (Suppl. table 4). The top ranked prognostic texture parameter, kurtosis in T1c images at filter level 2 (T1c_Kurtosis2), independently predicted reduced survival with a hazard ratio of 1.5 (1.2-2.0, p<0.001) when adjusted for high-risk status based on preoperative biopsy and MRI-measured tumor volume (Table 4). Significantly different recurrence- and progression-free survival was observed in patients based on the two highest ranked tumor texture parameters in the Cox analysis; T1c_Kurtosis2 and ADC_Entropy6 (also the best predictor of DMI) when grouping patients according to the textural tumor parameter </≥ median value (Figure 4a and b). The

proportion of patients given adjuvant treatment was higher in the poor outcome groups, with 51% versus 27% of the patients receiving adjuvant treatment in patients with T1c_Kurtosis2 ≥ median value versus < median value, respectively. Similarly, for patients with ADC_Entropy6 ≥ median value, 51% received adjuvant treatment compared to 26% in patients with ADC_Entropy6 < median value.

Discussion

In this large, population-based study we have demonstrated that texture parameters derived from preoperative MRI are significantly associated with high-risk disease and reduced survival in endometrial cancer. Our findings suggest that tumor texture analysis yields clinically relevant imaging markers that may aid in the preoperative staging and risk assessment.

Surgical staging and subsequent histological assessment have traditionally been the primary basis for treatment and prognostication in endometrial cancer, thereby allowing only limited risk stratification prior to surgery. In this study we link novel MRI features to established risk factors in endometrial cancer, and identify tumor texture parameters that non-invasively and very accurately predict high-risk status preoperatively. In multivariable analyses when adjusting for other relevant markers available preoperatively, the texture parameters remain significant and independent predictors of DMI and high-risk histological subtype. Similarly, in the survival analysis, the top ranked texture parameter is a significant and independent predictor of recurrence- and progression-free survival, comparable to MRI-measured tumor volume, which is previously reported as a strong prognostic factor (21).

Interestingly, a recent preliminary MRI study using TexRAD in endometrial cancer (10), found that a subset of 11 texture parameters jointly predicted DMI with an AU-ROC at 0.84, comparable to 0.81 for the top ranked single parameter in our study (ADC_Entropy6). However, a subset of 16 texture parameters jointly predicted high-grade tumor with an AU-

ROC at 0.83 (10), being higher than 0.66 for the top ranked single parameter in our study (T1c_MPP4). To our knowledge, our study is the first linking texture parameters to survival in endometrial cancer.

Among the texture features extracted by TexRAD (22) we found the parameters entropy, MPP and kurtosis to be the most promising biomarkers in endometrial cancer. As the texture features are pure mathematical descriptors of histogram shape, their biological correlates are somewhat unclear. However, entropy reflects textural irregularity and is clearly linked to heterogeneity. MPP is a TexRad specific feature, which in MRI is relevant only in filtered images, i.e. when pixels are recoded into a range of positive values or negative values according to their native values. Consequently, MPP reduces the impact of dark objects in the image, as elaborated in a review by Miles et. al. (22). Kurtosis reflects the shape of the histogram in terms of pointedness, taking into account the relation between centrum and periphery, i.e. high kurtosis typically reflects frequent extreme deviations, as opposed to frequent modestly sized deviations yielding lower kurtosis values. Hypothesized to enhance the biologically relevant information in medical images, the TexRad specific filtering-algorithm is based on Laplacian of Gaussian (LoG) spatial bandpass filtering with spatial scale filter (SSF) ranging from 2-6 mm, corresponding to objects of 2-6 mm in size, respectively (22). Among our top ranked predictors, we found texture parameters of all filter levels, often highly correlated. We did not see a clear pattern in which certain filter levels had a better predictive or prognostic performance than others. This observation complies with previous TexRad based publications, including the previous endometrial cancer study, in which no specific filter level has proven general superiority (10). Thus, our findings also illustrate some of the diversity and complexity of radiomics; characterizing cancers of different origin, type, subtype and grade, using images originating from different modalities and protocols and employing image analyses being inherently software- and operator-

dependent. Furthermore, a high number of extracted features increases the risk of overfitting statistical models.

In routine clinical practice, conventional MRI is widely established as a useful tool in the preoperative assessment of endometrial cancer. Adding texture analysis does not increase scan time, nor patient-related side effects. A PACS-integrated software like TexRAD enables high throughput texture analysis, with only a few minutes operator time per case. The decisive steps are image selection and tumor segmentation, which in our study were done manually. With advances in technology, semi-automated and automated tumor segmentation is increasingly available. However, this approach was not within the scope of our study. Extending the analysis from a two dimensional (2d) approach (largest cross-sectional tumor area) to a three dimensional (3d) approach (whole tumor) would also be more feasible if based on autosegmentation. One publication on CT texture analysis of colorectal cancer compared 2d to 3d approach and found 3d analysis to be slightly more representative of tumor heterogeneity and yielded better prognostic information (23). This was, however, a relatively small (n=55) and retrospective study, and the benefit of 3d approach should be further evaluated – also taking into account its time consuming nature.

Our study has some limitations. Firstly, the study was conducted in a single institution using a standardized imaging protocol. Thus, our results are not necessarily generally applicable to different scanners or patient populations. However, the imaging protocol was largely based upon ESUR guidelines and would be expected to be similar in clinical practice elsewhere. Secondly, intra- and interobserver variability for the texture measurements has not been assessed in this study, which was based on manual segmentation. Valid, automated tumor segmentation tools could potentially overcome interobserver variability, and this should be explored in future research. Lastly, the histogram based approach in TexRAD does

not cover all aspects of texture analysis. Our findings should encourage future research with even more sophisticated image texture analysis.

In summary, preoperative tumor texture analysis from MRI independently predicts high-risk disease and reduced survival in endometrial cancer. This novel approach using radiomics to yield prognostic biomarkers may ultimately guide tailored treatment in endometrial cancer. However, the value of image texture analysis in endometrial cancer needs to be further evaluated and validated across observers, centers and platforms, prior to potential implementation in clinic.

Reference List

1. Andor N, Graham TA, Jansen M, et al. Pan-cancer analysis of the extent and consequences of intratumor heterogeneity. Nat Med 2016; 22:105-113.

2. Morris LG, Riaz N, Desrichard A, et al. Pan-cancer analysis of intratumor heterogeneity as a prognostic determinant of survival. Oncotarget 2016; 7:10051-10063.

3. Gerlinger M, Rowan AJ, Horswell S, et al. Intratumor heterogeneity and branched evolution revealed by multiregion sequencing. N Engl J Med 2012; 366:883-892.

4. Gillies RJ, Kinahan PE, Hricak H. Radiomics: Images Are More than Pictures, They Are Data. Radiology 2016; 278:563-577.

5. Sala E, Mema E, Himoto Y, et al. Unravelling tumour heterogeneity using next-generation imaging: radiomics, radiogenomics, and habitat imaging. Clin Radiol 2017; 72:3-10.

6. Rose CJ, Mills SJ, O'Connor JP, et al. Quantifying spatial heterogeneity in dynamic contrast-enhanced MRI parameter maps. Magn Reson Med 2009; 62:488-499.

7. Ganeshan B, Goh V, Mandeville HC, Ng QS, Hoskin PJ, Miles KA. Non-small cell lung cancer: histopathologic correlates for texture parameters at CT. Radiology 2013; 266:326-336.

8. Ahmed A, Gibbs P, Pickles M, Turnbull L. Texture analysis in assessment and prediction of chemotherapy response in breast cancer. J Magn Reson Imaging 2013; 38:89-101.

9. Wibmer A, Hricak H, Gondo T, et al. Haralick texture analysis of prostate MRI: utility for differentiating non-cancerous prostate from prostate cancer and differentiating prostate cancers with different Gleason scores. Eur Radiol 2015; 25:2840-2850.

10. Ueno Y, Forghani B, Forghani R, et al. Endometrial Carcinoma: MR Imaging-based Texture Model for Preoperative Risk Stratification-A Preliminary Analysis. Radiology 2017; 284:748-757.

11. Amant F, Moerman P, Neven P, Timmerman D, Van LE, Vergote I. Endometrial cancer. Lancet 2005; 366:491-505.

12. Pecorelli S. Revised FIGO staging for carcinoma of the vulva, cervix, and endometrium. Int J Gynaecol Obstet 2009; 105:103-104.

13. Salvesen HB, Haldorsen IS, Trovik J. Markers for individualised therapy in endometrial carcinoma. Lancet Oncol 2012; 13:e353-e361.

14. Frei KA, Kinkel K. Staging endometrial cancer: role of magnetic resonance imaging. J Magn Reson Imaging 2001; 13:850-855.

15. Kinkel K, Forstner R, Danza FM, et al. Staging of endometrial cancer with MRI: guidelines of the European Society of Urogenital Imaging. Eur Radiol 2009; 19:1565-1574.

16. Sala E, Rockall AG, Freeman SJ, Mitchell DG, Reinhold C. The added role of MR imaging in treatment stratification of patients with gynecologic malignancies: what the radiologist needs to know. Radiology 2013; 266:717-740.

17. Haldorsen IS, Salvesen HB. Staging of endometrial carcinomas with MRI using traditional and novel MRI techniques. Clin Radiol 2012; 67:2-12.

18. Haldorsen IS, Husby JA, Werner HM, et al. Standard 1.5-T MRI of endometrial carcinomas: modest agreement between radiologists. Eur Radiol 2012; 22:1601-1611.

19. Silverberg RJ, Kurman RJ, Nogales F. Tumors of the uterine corpus. In: Tavassoli FA, Devilee P eds. Tumours of the Breast and Female Genital Organs. World Health Organization Classification of Tumours. Pathology & Genetics. Lyon, France: IACR Press Inc, 2003; 217-258.

20. Ytre-Hauge S, Husby JA, Magnussen IJ, et al. Preoperative tumor size at MRI predicts deep myometrial invasion, lymph node metastases, and patient outcome in endometrial carcinomas. Int J Gynecol Cancer 2015; 25:459-466.

21. Todo Y, Watari H, Okamoto K, et al. Tumor volume successively reflects the state of disease progression in endometrial cancer. Gynecol Oncol 2013; 129:472-477.

22. Miles KA, Ganeshan B, Hayball MP. CT texture analysis using the filtration-histogram method: what do the measurements mean? Cancer Imaging 2013; 13:400-406.

23. Ng F, Kozarski R, Ganeshan B, Goh V. Assessment of tumor heterogeneity by CT texture analysis: can the largest cross-sectional area be used as an alternative to whole tumor analysis? Eur J Radiol 2013; 82:342-348.

Table 1
Patient and tumor characteristics for 180 endometrial carcinoma patients studied.

Age, mean (range)	67 (41-93)
BMI, mean (range)	28 (16-50)
Postmenopausal, n (%)	166 (93%)
FIGO stage, n (%)	
IA	87 (48%)
IB	45 (25%)
II	21 (12%)
IIIB	3 (2%)
IIIC1	13 (7%)
IIIC2	7 (4%)
IVA	1 (1%)
IVB	3 (2%)
Histologic subtype, n (%)	
Endometrioid	142 (79%)
Clear cell	6 (3%)
Serous	19 (11%)
Carcinosarcoma	9 (5%)
Undifferentiated/others	4 (2%)
Histological grade in endometrioid tumors, n (%)	
Grade 1	64 (45%)
Grade 2	46 (32%)
Grade 3	30 (21%)

FIGO stage refers to the International Federation of Gynecology and Obstetrics stage according to 2009 criteria.
BMI, body mass index.

Table 2
Top ranked MRI derived texture parameters in relation to clinical and histological characteristics in 180 endometrial carcinoma patients.

	ADC_Entropy6 [a]			T2_MPP4 [b]			T1c_Entropy6 [c]			T1c_MPP4 [d]			T1c_Kurtosis2 [e]		
Variable	n	Median (95% CI)	p*	n	Median (95% CI)	p*	n	Median (95% CI)	p*	n	Median (95% CI)	p*	n	Median (95% CI)	p*
Myometrial invasion			**<0.001**			**<0.001**			**<0.001**			**<0.001**			**0.001**
<50%	99	3.8 (3.6-4.0)		100	242 (200-260)		100	4.5 (4.3-4.8)		100	92 (71-110)		100	0.04 (-0.22-0.26)	
≥50%	76	4.7 (4.6-5.0)		78	140 (124-160)		78	5.4 (5.2-5.6)		78	141 (121-170)		78	0.42 (0.24-0.67)	
Cervical stromal invasion			0.02			0.01			0.03			0.10			0.01
No	144	4.1 (3.9-4.3)		146	192 (173-212)		146	4.9 (4.6-5.0)		146	110 (92-122)		146	0.14 (0.00-0.28)	
Yes	31	4.7 (4.4-5.0)		32	135 (105-221)		32	5.3 (4.8-5.6)		32	138 (94-186)		32	0.55 (0.31-0.91)	
Lymph node metastases			0.004			0.01			**0.001**			0.13			0.03
No	132	4.2 (4.0-4.4)		135	190 (174-205)		135	4.9 (4.6-5.0)		135	111 (94-124)		135	0.16 (0.00-0.30)	
Yes	19	5.1 (3.9-5.5)		19	133 (105-223)		19	5.8 (4.7-6.2)		19	141 (92-186)		19	0.58 (0.06-1.12)	
Histological type/grade			**0.001**			0.01			**<0.001**			**<0.001**			0.02
E1+2	109	4.0 (3.9-4.3)		110	192 (173-239)		110	4.8 (4.5-5.0)		110	98 (81-118)		110	0.07 (-0.11-0.28)	
E3+NE	66	4.6 (4.3-4.9)		68	162 (132-192)		68	5.3 (4.9-5.5)		68	143 (112-174)		68	0.46 (0.26-0.62)	
Age			0.21			0.03			0.17			0.01			0.07
<67	90	4.1 (4.0-4.4)		90	193 (173-228)		90	4.9 (4.6-5.0)		90	99 (81-114)		90	0.13 (-0.10-0.33)	
≥67 (median and above)	87	4.4 (4.0-4.6)		90	173 (143-200)		90	5.0 (4.8-5.3)		90	127 (112-150)		90	0.29 (0.13-0.58)	
BMI			0.63			0.89			0.61			0.83			0.70
<25	50	4.4 (3.9-4.7)		50	177 (160-207)		50	4.9 (4.6-5.3)		50	115 (82-146)		50	0.29 (-0.10-0.48)	
≥25 (overweight)	124	4.2 (4.0-4.4)		126	185 (158-205)		126	4.9 (4.7-5.1)		126	113 (100-134)		126	0.22 (0.03-0.35)	

* Mann-Whitney U Test.

[a] Highest ranked texture parameter for prediction of myometrial invasion.

[b] Highest ranked texture parameter for prediction of cervical stroma invasion.

[c] Highest ranked texture parameter for prediction of lymph node metastases.

[d] Highest ranked texture parameter for prediction of histological type/grade.

[e] Highest ranked texture parameter for prediction of recurrence- and progression-free survival.

Significant p values after modified Bonferroni correction (<0.002) are given in **bold**.

ADC, apparent diffusion coefficient (maps); BMI, body mass index; CI, confidence interval; E1-3, endometrioid grade 1-3; MPP, Mean of positive pixels; MRI, magnetic resonance imaging; NE, non-endometrioid; T1c, contrast enhanced T1-weighted (images); T2, T2-weighted (images).

Table 3
Univariable and multivariable logistic regression for prediction of deep myometrial invasion, cervical stroma invasion, lymph node metastases and high-risk histological subtype at surgical staging. The top ranked texture parameter is included in each category.

		Univariable		Multivariable	
Dependent variable (based on surgical staging/pathology)	Predicting variable (from preoperative imaging and biopsy)	Unadjusted OR (95% CI)	p	Adjusted§ OR (95% CI)	p
Deep myometrial invasion	ADC_Entropy6	4.7 (2.8-7.8)	**<0.001**	3.2 (1.7-6.1)	**<0.001**
	MRI tumor volume	1.05 (1.03-1.07)	**<0.001**	1.01 (0.99-1.03)	0.36
	MRI reading DMI+	5.3 (2.8-10.1)	**<0.001**	2.0 (0.9-4.4)	0.08
	High-risk biopsy*	1.2 (0.6-2.2)	0.66	0.7 (0.3-1.6)	0.41
Cervical stroma invasion	T2_MPP4	0.995 (0.99-1.00)	0.03	0.996 (0.99-1.00)	0.11
	MRI tumor volume	1.006 (1.00-1.01)	0.02	0.999 (0.99-1.01)	0.77
	MRI reading CSI+	6.2 (2.3-16.6)	**<0.001**	4.5 (1.4-14.3)	**0.01**
	Biopsy Cervix+	2.2 (1.2-3.9)	0.01	2.0 (1.1-3.9)	**0.03**
Lymph node metastases	T1c_Entropy6	3.1 (1.5-6.6)	0.003	1.7 (0.7-4.3)	0.26
	MRI tumor volume	1.02 (1.01-1.03)	0.007	1.01 (0.99-1.03)	0.43
	MRI reading LNM+	23.8 (6.2-91.8)	**<0.001**	14.0 (3.2-61.0)	**<0.001**
	High-risk biopsy*	3.0 (1.1-8.0)	0.03	1.6 (0.5-5.2)	0.45
High-risk histological subtype*	T1c_MPP4	1.01 (1.00-1.01)	**0.001**	1.01 (1.00-1.01)	**0.004**
	MRI tumor volume	1.02 (1.01-1.04)	**<0.001**	1.02 (1.00-1.04)	**0.02**
	High-risk biopsy*	22.7 (9.5-54.4)	**<0.001**	24.6 (9.6-63.5)	**<0.001**

* High-risk-histological subtype is defined as endometrioid grade 3 or non-endometrioid subtype as opposed to low-risk histological subtype defined as endometrioid grade 1 and 2.

§ All variables grouped by vertical leaders are included in each multivariable analysis.

Significant p values (after modified Bonferroni correction in univariable analysis ($p<0.002$) and $p<0.05$ in multivariable analysis) are given in **bold.**

ADC, apparent diffusion coefficient (maps); CI, confidence interval; CSI, cervical stroma invasion; LNM, lymph node metastases; MPP, Mean of positive pixels; MRI, magnetic resonance imaging; OR, odds ratio; T1c, contrast enhanced T1-weighted (images); T2, T2-weighted (images).

Table 4
Univariable and multivariable Cox regression analysis for prediction of recurrence- and progression-free survival.

		Univariable		Multivariable	
Dependent variable	Predicting variable (covariates)	Unadjusted HR (95% CI)	p	Adjusted[§] HR (95% CI)	p
RPFS	T1c_Kurtosis2	1.7 (1.3-2.3)	**<0.001**	1.6 (1.2-2.1)	**0.003**
	T1c_Entropy6	2.1 (1.4-3.2)	**<0.001**	0.7 (0.2-2.5)	0.61
	ADC_Entropy6	2.0 (1.4-2.9)	**<0.001**	2.1 (0.7-6.3)	0.17
RPFS	T1c_Kurtosis2	1.7 (1.3-2.3)	**<0.001**	1.5 (1.2-2.0)	**<0.001**
	MRI tumor volume	1.01 (1.00-1.01)	**<0.001**	1.01 (1.00-1.01)	**0.007**
	High-risk biopsy*	4.3 (2.3-8.0)	**<0.001**	3.4 (1.8-6.4)	**<0.001**

* Categorical variable. High-risk biopsy is defined as endometrioid grade 3 or non-endometrioid subtype as opposed to low-risk comprising endometrioid grade 1 and 2.

[§] All variables grouped by vertical leaders are included in each multivariable analysis.

Significant p values (after modified Bonferroni correction in univariable analysis ($p<0.002$) and $p<0.05$ in multivariable analysis) are given in **bold**.

ADC, apparent diffusion coefficient (maps); CI, confidence interval; HR, hazard ratio; MRI, magnetic resonance imaging; RPFS, recurrence- and progression-free survival; T1c, contrast enhanced T1-weighted (images).

Suppl. table 1
Spearman correlation coefficients (r_s) for the top ranked texture parameters in table 2 at different filter levels (SSF 0-6).

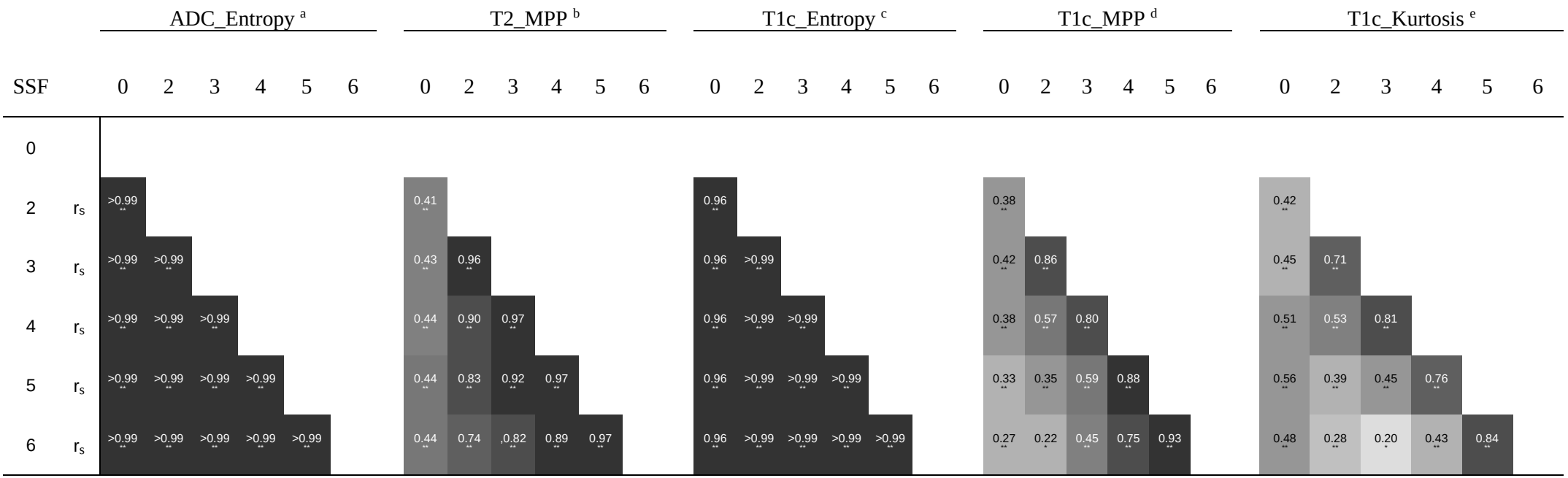

** Correlation is significant at the 0.002 level (2-tailed).
* Correlation is significant at the 0.05 level (2-tailed).

[a] ADC_Entropy6 was the highest ranked texture parameter for prediction of myometrial invasion.

[b] T2_MPP4 was the highest ranked texture parameter for prediction of cervical stroma invasion.

[c] T1c_Entropy6 was the highest ranked texture parameter for prediction of lymph node metastases.

[d] T1c_MPP4 was the highest ranked texture parameter for prediction of histological type/grade.

[e] T1c_Kurtosis2 was the highest ranked texture parameter for prediction of recurrence- and progression-free survival.

ADC, apparent diffusion coefficient (maps); MPP, Mean of positive pixels; SSF, spatial scale of filtration; T1c, contrast enhanced T1-weighted (images); T2, T2-weighted (images).

Suppl. table 2
Range of Spearman correlation coefficients (r_s) among texture parameters of different filter levels (SSF 0-6).

	Standard deviation	Entropy	Skewness	MPP	Kurtosis
	r_s	r_s	r_s	r_s	r_s
T1c	0.35 – 0.91	0.96 – 1.00	0.00 – 0.87	0.22 – 0.93	0.20 – 0.84
T2	0.50 – 0.95	0.86 – 0.99	0.14 – 0.88	0.41 – 0.97	0.32 – 0.87
ADC	0.60 – 0.96	0.99 – 1.00	0.18 – 0.90	0.29 – 0.91	0.29 – 0.91

ADC, apparent diffusion coefficient (maps); MPP, Mean of positive pixels; SSF, spatial scale of filtration; T1c, contrast enhanced T1-weighted (images); T2, T2-weighted (images).

Suppl. table 3
Range of Spearman correlation coefficients (r_s) among texture parameters from MR images (T1c/T2/ADC) at the same filter level (SSF).

	Standard deviation	Entropy	Skewness	MPP	Kurtosis
	r_s	r_s	r_s	r_s	r_s
T1c/T2/ADC	0.18 – 0.46	0.76 – 0.95	-0.17 – 0.30*	-0.48 – 0.35**	0.10 – 0.37

* Lowest absolute value: 0.00

** Lowest absolute value: 0.02

ADC, apparent diffusion coefficient (maps); MPP, Mean of positive pixels; MR, magnetic resonance; SSF, spatial scale of filtration; T1c, contrast enhanced T1-weighted (images); T2, T2-weighted (images).

Suppl. table 4
Top 10 ranked MRI derived texture parameters for predicting clinical and histological characteristics and survival in 180 endometrial carcinoma patients.

	Deep myometrial invasion (Yes/No)		Cervical stroma invasion (Yes/No)		Lymph node metastases (Yes/No)		Histological grade (E1+E2 vs E3+NE)		Recurrence- and progression-free Survival	
Rank	Texture parameter	p*	Texture parameter	p*	Texture parameter	p*	Texture parameter	p*	Texture parameter	p+
1	ADC_Entropy6	**3.02×10^{-12}**	T2_MPP4	0.0119	T1c_Entropy6	**0.00114**	T1c_MPP4	**0.000297**	T1c_Kurtosis2	**0.000027**
2	ADC_Entropy4	**3.59×10^{-12}**	T2_MPP3	0.0125	T1c_Entropy5	**0.00144**	T1c_MPP5	**0.000692**	ADC_Entropy6	**0.000148**
3	ADC_Entropy3	**3.66×10^{-12}**	ADC_Entropy4	0.0131	T1c_Entropy2	**0.00150**	T1c_Entropy0	**0.000741**	ADC_Entropy4	**0.000149**
4	ADC_Entropy2	**3.82×10^{-12}**	T1c_Kurtosis2	0.0139	T1c_Entropy3	**0.00147**	T1c_Entropy6	**0.000786**	ADC_Entropy2	**0.000150**
5	ADC_Entropy5	**3.99×10^{-12}**	ADC_Entropy2	0.0139	T1c_Entropy4	**0.00167**	T1c_MPP3	**0.000821**	ADC_Entropy3	**0.000155**
6	ADC_Entropy0	**5.32×10^{-12}**	ADC_Entropy3	0.0144	ADC_Entropy0	0.00314	T1c_Entropy3	**0.000834**	ADC_Entropy5	**0.000168**
7	T1c_Entropy0	**6.01×10^{-12}**	ADC_Entropy5	0.0149	T1c_Entropy0	0.00315	T1c_Entropy2	**0.000848**	ADC_Entropy0	**0.000308**
8	T1c_Entropy6	**1.43×10^{-11}**	ADC_Entropy6	0.0151	ADC_Entropy2	0.00322	T1c_Entropy5	**0.000867**	T1c_Entropy6	**0.000446**
9	T1c_Entropy5	**2.37×10^{-11}**	T2_MPP2	0.0170	ADC_Entropy4	0.00325	T1c_Entropy4	**0.000876**	T1c_Entropy5	**0.000581**
10	T1c_Entropy2	**3.81×10^{-11}**	T1c_Entropy0	0.0174	ADC_Entropy3	0.00331	ADC_Entropy5	**0.001125**	T1c_Entropy4	**0.000626**

* Mann-Whitney U Test.

+ Univariable Cox regression analysis.

Texture parameters differing only in filter level (SSF 0-6) are grouped by colors.

Significant p values after modified Bonferroni correction (<0.002) are given in **bold**.

ADC, apparent diffusion coefficient (maps); E1-3, endometrioid grade 1-3; MPP, Mean of positive pixels; MRI, magnetic resonance imaging; NE, non-endometrioid; SSF, spatial scale of filtration; T1c, contrast enhanced T1-weighted (images); T2, T2-weighted (images).

Figure legends

Figure 1

Endometrial carcinoma manually segmented (blue line) on contrast-enhanced T1-weighted (T1c) image (upper row), T2-weighted (T2) image (middle row) and ADC-map (lower row) from the same 52-year old postmenopausal woman diagnosed with stage 1b endometrial cancer (endometrioid, grade 1). Successive filtered images (spatial scale of filtration (SSF) 2-6) to the right of each native image.

Figure 2

Proportions of the respective texture parameters predicting presence of deep myometrial invasion, cervical stroma invasion, lymph node metastases and high-risk histological subtype at significance level of 0.05 (a) and at significance level of 0.002 (b) are given in the bars. Upwards arrows indicate that high values for the respective texture parameter predict positive staging parameters/high-risk status whereas downwards arrows indicate that low values for the respective texture parameters predict positive staging parameters/high-risk status.
ADC, apparent diffusion coefficient (maps); MPP, mean of positive pixels; SD, standard deviation; T1c, contrast-enhanced T1-weighted (images); T2, T2-weighted (images).

Figure 3

Receiver operator characteristics (ROC)-curves visualizing the diagnostic performance of the top ranked texture parameters for predicting presence of the staging parameters deep myometrial invasion (a), cervical stroma invasion (b), lymph node metastases (c) and for high-risk histological subtype (d). ADC_entropy6 yielded an area under the curve (AUC) of

0.81 ($p<0.001$) for prediction of deep myometrial invasion (a), T2_MPP4 an AUC of 0.64 ($p=0.01$) for prediction of cervical stroma invasion (b), T1c_Entropy6 and AUC of 0.73 ($p=0.001$) for prediction of lymph node metastases (c) and T1c_MPP4 and AUC of 0.66 ($p<0.001$) for prediction of high-risk histological subtype (d). P values refer to the test of equal areas under the diagonal and the ROC-curve.

Figure 4

Kaplan-Meier curves depicting significantly different patient survival for the two highest ranked tumor texture parameters: T1c_Kurtosis2 (a) and ADC_Entropy6 (b). High tumor values for T1c_Kurtosis2 (a) and for ADC_Entropy6 (b) were significantly associated with reduced recurrence- and progression free survival ($p=0.0004$ and $p=0.004$, respectively). P values refer to the Mantel-Cox (log-rank) test.